10 November 2000

ELSEVIER

Chemical Physics Letters 330 (2000) 403–409

CHEMICAL PHYSICS LETTERS

www.elsevier.nl/locate/cplett

# Subpicosecond study of excitons in a phenylenevinylene conjugated polymer: exciton–exciton interactions and infrared photoinduced absorption features

B. Kraabel *, D.W. McBranch

*Chemical Science and Technology Division, CST-6, MS-J567, Los Alamos National Laboratory, Los Alamos, NM 87545, USA*

Received 5 July 2000

**Abstract**

We present a study of the fundamental photoexcitations in a phenylenevinylene conjugated polymer from the visible to the mid-infrared (IR) using polarized subpicosecond transient absorption (TA) spectroscopy. From 0.5 to roughly 1.3 eV we find that features due to singlet intrachain excitons dominate the photoinduced absorption. Two peaks are apparent in the spectrum: one near 0.5 eV and the other at ~1.1 eV. In the regime of high excitation densities ($>10^{19}$ cm$^{-3}$), we find evidence of exciton–exciton interactions leading to exciton hopping between different chains or segments of the polymer. © 2000 Published by Elsevier Science B.V.

## 1. Introduction

Conjugated phenylene-based polymers have attracted significant interest over the last decade due to their promise in optoelectronic applications such as light-emitting diodes, [1,2] and solid-state lasers [3,4]. Optimizing device design requires a thorough understanding of the fundamental photophysics of these materials, particularly as regards mechanisms which affect the photoluminescence efficiency. Subpicosecond transient spectroscopy has proved an effective method for studying the photophysics of these materials [5–8] specifically because the time resolution allows one to monitor the photoexcitations before (or while) secondary effects take place, such as spectral diffusion or the formation of secondary species. Hence a clearer picture of the relaxation pathways, branching ratios and generation and interaction mechanisms of the photo-excitations may be formed.

We present the results of polarized transient absorption (TA) studies on poly(2,3-diphenyl-5-hexyl-*p*-phenylenevinylene) (DP6-PPV), from the visible to the mid-infrared (IR). This material is attractive for applications requiring large optical gain because of its long-lived stimulated emission (SE) band [9]. We report the existence of a TA band in the IR which is associated with the intrachain singlet exciton. The TA of the singlet exciton is highly anisotropic at excitation densities below saturation for excitons, but becomes isotropic within 300 fs once excitation densities exceed this limit. We interpret this as due to exciton–exciton interactions leading to interchain exciton hopping.

* Corresponding author. Present address: ViewGate Networks, 165 High Street, Sevenoaks, TN13 1XJ, UK. Fax: +44 1732 466401.

*E-mail address:* brett.kraabel@viewgate.com (B. Kraabel).

0009-2614/00/$ - see front matter 
PII: S0009-2614(00)00994-5

## 2. Experimental

The films of DP6-PPV were spun cast in an inert atmosphere from a $5 \times 10^{-3}$ M chloroform solution onto sapphire substrates. The high refractive index of sapphire ensured that no waveguiding took place in the polymer film, thus avoiding possible complications due to ASE [3]. To minimize the effects of photo-oxidation the samples were mounted in an optical cryostat in the dry box and all the experiments were carried out in a dynamic vacuum of $10^{-5}$ Torr at 77 K. The films were optically thin at the excitation wavelength, ensuring that the photoexcitation density was uniform throughout the film thickness.

The chirp-free TA setup used for these measurements has been described in detail elsewhere [10]. Briefly, it consists of a standard pump–probe setup optimized to allow acquisition of chirp-free TA spectra and sensitive to differential signals as small as $10^{-5}$. The pump photon energy of 3.1 eV was resonant with the $\pi$–$\pi^*$ absorption band of DP6-PPV (see arrow in inset to Fig. 1). In the visible and near IR the probe pulses were obtained via continuum generation in a sapphire plate, and passed through a calcite prism polarizer to ensure proper polarization.

For measurements in the mid-IR (1.0–0.5 eV) the output of an IR-pumped OPA (Clark MXR) was used. The probe pulses were linearly polarized either S or P (depending on whether we were using the signal or idler from the OPA or the continuum) using a calcite prism polarizer. The large dispersion of the calcite prism polarizer led to a time resolution of approximately 300 fs throughout the entire spectrum covered (visible to mid-IR). The polarization state of the pump pulses was adjusted either parallel or perpendicular to the probe pulses with a second calcite prism polarizer, followed by a computer-controlled half-wave plate. Unless otherwise stated, all measurements reported here were made with the pump and probe polarization vectors parallel.

As a measure of transmission changes we use the differential transmission (DT), which is defined as $\mathrm{DT} = (T - T_0)/T_0 = \Delta T/T_0$, where $T_0$ and $T$ are the transmission of the probe beam in the presence and absence of the pump, respectively. The pump–induced absorption change $\Delta\alpha$ is related to DT by the expression $\Delta\alpha = -(1/d)\ln(1 + \mathrm{DT})$ where $d$ is the sample thickness. In the small-signal regime in which we operated, $\Delta\alpha d \sim -\Delta T/T_0$.

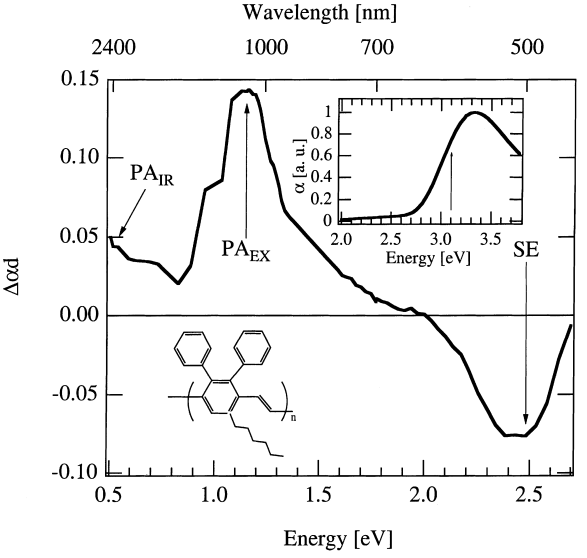


Fig. 1. TA spectrum of DP6-PPV at less than 1 ps pump–probe time delay, using an initial exitation density of $10^{18}$ cm$^{-3}$. The arrows labeled $PA_{IR}$, $PA_{EX}$ and SE denote the energy where the single wavelength measurements were made. The insets show the chemical structure of DP6-PPV and the linear absorption spectrum. The vertical arrow on the linear absorption spectrum denotes the pump wavelength used in these experiments.

The anisotropy of the TA signal is analyzed using the polarization anisotropy ratio $r(t)$, defined as [11]

$$r(t) = \frac{\Delta\alpha_{\parallel}(t) - \Delta\alpha_{\perp}(t)}{\Delta\alpha_{\parallel}(t) + 2\Delta\alpha_{\perp}(t)}, \tag{1}$$

where $\Delta\alpha_{\parallel}(t)$ $[\Delta\alpha_{\perp}(t)]$ is the absorption change with the pump polarization vector parallel (perpendicular) to the probe polarization vector. For an isotropic system containing non-interacting emitters, $r(t)$ is determined by the molecular absorption and emission tensors. For a disordered collection of linearly polarized chromophores, $r(t)$ can range from a maximum theoretical value of 0.4 for a highly anisotropic photoinduced absorption transition to 0 for a completely isotropic transition.

It is known that the linear absorption coefficient of conjugated polymers is at least two orders of magnitude greater along the chain direction than perpendicular to the chain direction [12,13]. Hence, in our measurements the linearly polarized pump pulses selectively excite chains which are (locally) parallel to the pump polarization vector. This means that the maximum anisotropy of 0.4 corresponds to the absorption dipole moment of the excited state being aligned along the (local) polymer backbone. As the absorbing or emitting species diffuse along the polymer chain or hop to neighboring chains, the orientational memory is lost, leading to a decrease in the anisotropy as a function of time.

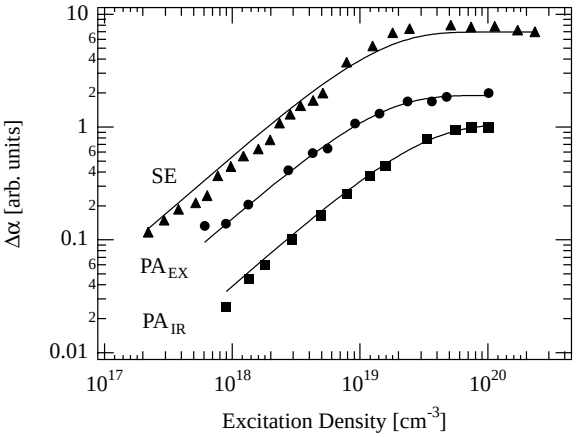


Fig. 2. The dependence of the three TA features shown in Fig. 1 on the excitation density, at approximately 200 fs pump–probe delay time.

## 3. Results

The chirp-free TA spectrum of DP6-PPV at less than 1 ps pump–probe delay time, for an excitation density of $10^{18}$ cm$^{-3}$, is shown in Fig. 1. For the purposes of discussion, we have labeled several spectral regions on Fig. 1. The region of negative TA is attributed to SE since it occurs in a spectral region with no linear absorption. We find that the SE spectrum at this excitation density exactly matches the photoluminescence spectrum, in agreement with earlier results [14]. The feature PA$_{EX}$ appears to be a generic feature of phenylene-based conjugated polymers, as discussed in a separate publication [9], and corresponds to the photoinduced absorption from singlet intrachain excitons to higher excited states. The feature marked PA$_{IR}$ is a new feature, and will be discussed in detail below. The spectral energies used for single-wavelength measurements of these features are 0.5, 1.15 and 2.5 eV for PA$_{IR}$, PA$_{EX}$ and SE, respectively.

The dependence of the various TA features on the excitation density at the peak of the TA signal is shown in Fig. 2. The solid triangles, circles and squares show the results obtained for the SE, PA$_{EX}$ and PA$_{IR}$, respectively. The solid lines are fits using the expression

$$\mathrm{TA}(\Phi) \propto \left(1 - \mathrm{e}^{-\Phi/\Phi_0}\right), \qquad (2)$$

where $\Phi$ represents the excitation density and $\Phi_0$ is the saturation density. These fits yield an identical saturation density of $\Phi_0 = 2 \pm 1 \times 10^{19}$ cm$^{-3}$ for the SE, PA$_{EX}$ and PA$_{IR}$.

The dynamics of PA$_{EX}$ and PA$_{IR}$ are shown in Fig. 3. The open and solid squares show the results obtained with an initial excitation density of $10^{19}$ cm$^{-3}$ for PA$_{EX}$ and PA$_{IR}$, respectively, while

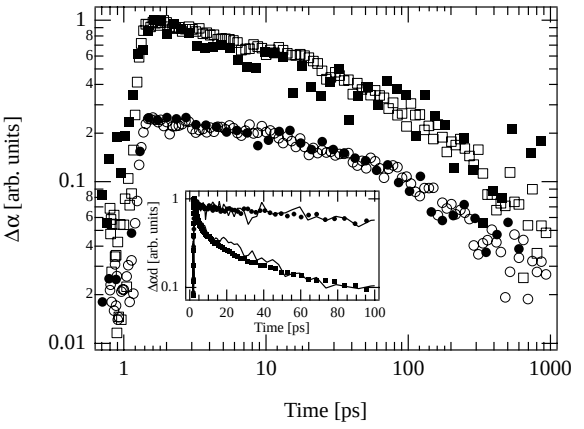


Fig. 3. The dynamics of PA$_{IR}$ (solid symbols) and PA$_{EX}$ (open symbols) for excitation densities of $10^{18}$ (circles) and $10^{19}$ (squares) cm$^{-3}$. The data (and the time axis) are offset for clarity. The inset shows the dynamics of PA$_{EX}$ (symbols) and and the SE (solid lines) for excitation densities of $10^{17}$ and $10^{19}$ cm$^{-3}$.

the open and solid circles show the results for an excitation density of $10^{18}$ cm$^{-3}$ for $PA_{EX}$ and $PA_{IR}$, respectively. A poor signal-to-noise ratio prevented measuring the dynamics of $PA_{IR}$ at lower excitation densities. The dynamics of $PA_{EX}$ and $PA_{IR}$ are clearly identical over three orders of magnitude in time for these two excitation densities. The inset to Fig. 3 shows the dynamics of $PA_{EX}$ (solid symbols) and the SE (solid lines) for initial excitation densities of $10^{17}$ and $10^{19}$ cm$^{-3}$. The dynamics of $PA_{EX}$ and SE are also clearly identical.

The anisotropy of $PA_{EX}$ as a function of pump–probe delay time is shown in Fig. 4a for excitation densities of $10^{17}$ (open squares), $10^{18}$ (open circles) and $10^{19}$ (solid triangles) cm$^{-3}$. The difference in the time dependence of the anisotropy below and above the saturation density is quite dramatic. Below the saturation density ($10^{17}$ and $10^{18}$ cm$^{-3}$) the anisotropy changes very little on the picosecond time scale from its initial value of ~0.4. Once saturation density is reached ($10^{19}$ cm$^{-3}$), however, the anisotropy decays very rapidly within the first picosecond from a value near 0.4 to approximately 0.2. Since this decay is on the time scale of the pulse width, the following formalism is used to fit the data [15]:

$$r(\tau) \propto \int_{-\infty}^{\infty} \mathrm{d}t\, I_{\mathrm{pb}}(t-\tau) \int_{-\infty}^{t} \mathrm{d}t'\, R(t'-t) I_{\mathrm{pp}}(t'), \quad (3)$$

$$R(t) = \Theta(t) \mathrm{e}^{(-t/\tau_a)}, \quad (4)$$

where $I_{\mathrm{pp}}(T)$ $[I_{\mathrm{pb}}(t)]$ represents the pump (probe) temporal profile and is modeled using a $\mathrm{sech}^2(2.269/\tau)$ function with a pulse width of $\tau = 300$ fs, $R(t)$ is the response function describing the system response, and $\Theta(t)$ is the Heavyside function. The initial fast decay of the anisotropy at high excitation density in Fig. 4 may be characterized using a monoexponential response function with a time constant $\tau_a$ of approximately 300 fs (see solid line in Fig. 4a).

The dynamics of the anisotropy the 100 ps time scale are shown in Fig. 4b, where we plot the results for excitation densities of $10^{17}$ (open squares), $10^{18}$ (open circles) and $10^{19}$ (solid triangles) cm$^{-3}$. For clarity, we shifted the time zero of this plot by 0.4 ps. On the 100 ps time scale the decay of the anisotropy below the saturation density (open circles) may be characterized by a monoexponential with a time constant of 20 ps (upper solid line in Fig. 4b). The dynamics of the anisotropy decay at the saturation excitation density (solid triangles) is best fit using a double exponential, with a fast time constant of 300 fs and a slower time constant of 3 ps. This fit is shown in Fig. 4b (lower solid line).

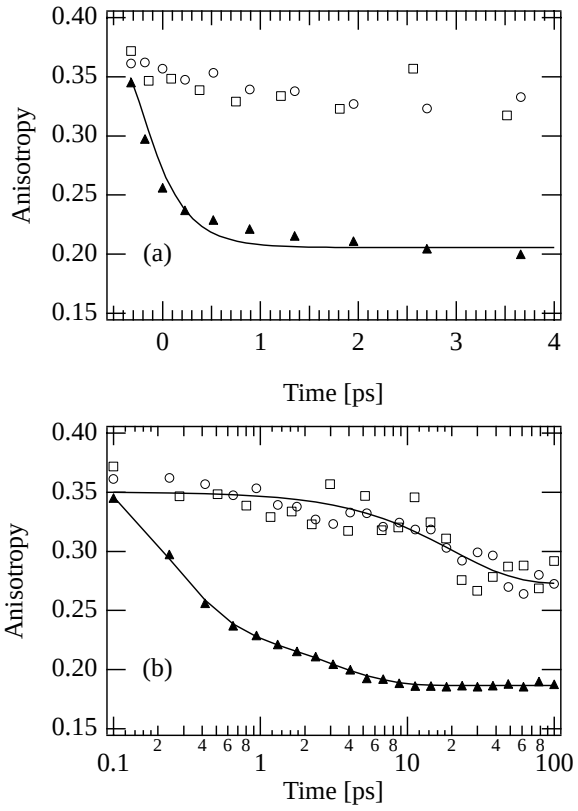


Fig. 4. Panel (a) shows the anisotropy of $PA_{EX}$ versus pump–probe delay time using excitation densities of $10^{17}$ (open squares), $10^{18}$ (open circles) and $3 \times 10^{19}$ (solid triangles) cm$^{-3}$. The solid line is a fit to a monoexponential using Eq. (3), and yields a time constant of 300 fs. Panel (b) shows the data for excitation densities of $10^{18}$ (open circles) and $3 \times 10^{19}$ (solid triangles) cm$^{-3}$. The upper solid line is a fit to a monoexponential with a time constant of 20 ps, while the lower solid line is a fit to a double exponential with time constants of 300 fs and 3 ps.

Fig. 5 shows the anisotropy of $PA_{EX}$ at a 2 ps pump–probe delay time as a function of excitation density. The solid line in Fig. 5 is a fit to

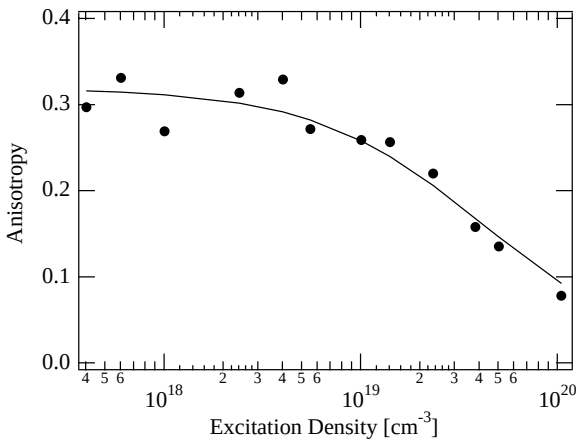


Fig. 5. The anisotropy of $PA_{EX}$ at a pump–probe delay time of 2 ps as a function of intitial excitation density. The solid line is a fit using Eq. (5), and yields a saturation density of $\sim 10^{19}$ cm$^{-3}$.

$$r(\Phi) = \frac{B\Phi_0}{\Phi_0 + \Phi}, \tag{5}$$

where $\Phi$ represents the initial photoexcitation density and $\Phi_0$ represents the saturation density. The fit yields a saturation density of $\sim 10^{19}$ cm$^{-3}$, similar to the saturation density found for the TA (see Fig. 2). The results for the anisotropy of $PA_{IR}$ are identical to the results for $PA_{EX}$.

## 4. Discussion

### 4.1. Transient absorption in the IR

We report the existence of a TA feature in the IR in DP6-PPV, which we have labeled $PA_{IR}$ in Fig. 1. This feature shares the same dynamics, excitation density dependence and dynamic anisotropy as $PA_{EX}$. The dynamics of the TA from 0.5 eV to approximately 1.3 eV are identical, implying that a single photoexcited species dominates this part of the TA spectrum from 100 fs to 100 ps time scale. Since $PA_{EX}$ is known to be due to a transition from singlet intrachain excitons ($^1B_u$) to higher excited states ($^mA_g$) [9], we conclude that $PA_{IR}$ is also due to a transition from singlet intrachain excitons to higher excited states ($^kA_g$) that lie approximately 0.5 eV below the $^mA_g$ states.

Previous publications reported a TA feature in the IR in different PPV derivatives, also peaking near 0.5 eV [7,16]. However, the spectral range of these measurements did not include the region between approximately 0.5 and 1 eV, but instead covered the range below 0.5 eV, and above approximately 1 eV. The present work bridges this gap and shows that the IR feature observed in these earlier works indeed peaks near 0.5 eV.

The assignment of $PA_{IR}$ to the exciton is in agreement with Frolov et al. [16] who also found matching dynamics for $PA_{IR}$ and $PA_{EX}$ in a soluble PPV derivative. In contrast, Hsu and coworkers assign the IR feature they observe in a substituted PPV to a charge-separated species [7]. However, their assignment is based on the matching dynamics of the red tail of the $PA_{IR}$ feature (at 0.29 eV) with those of the TA feature at 1.5 eV. Hence it is not clear from their published results whether the entire $PA_{IR}$ band follows the same dynamics as the visible TA band. Results obtained in our laboratory with a different phenylene-based conjugated polymer, poly(9,9-dioctylfluorene) (PFO), indicate that two distinct PA bands exist near 0.5 eV in this material, with the lower energy band decaying more slowly than the higher energy band [17]. In view of the fact that the charge-separated species ($PA_{CS}$) decays more slowly than the excitons ($PA_{EX}$), and the similarity of many phenylene-based conjugated polymers [9], these results in PFO suggest the possibility that another $PA_{IR}$ band may exist in DP6-PPV, but below the minimum probe energy of this measurement (0.5 eV).

Further comparison of the $PA_{IR}$ band observed in this work with that observed by Hsu et al. [7] is hindered due to the different experimental parameters. For example, the TA spectrum published by Hsu et al. is for a 200 ps pump–probe delay time, leaving open the question of how the spectrum evolves over the first 200 ps. In addition, no mention of the excitation density used is made in their report, although it is now established that excitation density plays a significant role in determining the branching ratio between excitons and charge separated photoexcitations [6,9]. In the work of Hsu et al. they show that the dynamics of the SE do not match those of $PA_{EX}$, which is generally considered a sign of either a degraded sample, or excitation densities above the satura-

tion limit for singlet intrachain excitons [9]. Thus, although it is apparent from their results that a TA band exists in the IR which is related to a charge separated species, the observation of this band may depend on the quality of the sample used and on the excitation density used. In the present work, no evidence is found to relate $PA_{IR}$ to $PA_{CS}$ (the charge separated species) in DP6-PPV films.

### 4.2. Anisotropy of $PA_{EX}$

We find that the dynamic anisotropy of the $PA_{EX}$ (and the $PA_{IR}$) feature is the same as for the SE. The $PA_{EX}$ and $PA_{IR}$ features are due to transitions from singlet intrachain excitons to higher excited states, while SE (and luminescence) is due to transitions from singlet excitons back to the ground state. Hence we expect the anisotropy of $PA_{EX}$ and $PA_{IR}$ to be very similar to that of the stimulated emission, provided the extension along the polymer backbone of the upper excited state involved in the TA transition is similar to that of the ground state. Thus our results indicate that the higher excited states involved in the $PA_{EX}$ or $PA_{IR}$ transitions are extended states that are strongly oriented along the polymer backbone.

At low excitation densities the anisotropy of $PA_{EX}$ decays on the 10 ps time scale from an initial value of near 0.4 to approximately 0.25, in agreement with previous work on substituted PPVs [18]. As discussed above, an anisotropy near 0.4 implies that the $PA_{EX}$ transition dipole moment is essentially aligned along segments of the polymer backbone that are parallel to the pump polarization vector. The change in the anisotropy can result only from exciton migration, either by diffusion or energy transfer, to different chains, or to segments of the same chain with a different (local) chain direction. Exciton decay into secondary species that do not have transitions in the spectral region of $PA_{EX}$ will not affect the aniostropy of the $PA_{EX}$ feature.

We find that the time scale of the decay of the $PA_{EX}$ anisotropy is similar to that observed for the dynamic red-shift of the luminescence in films of PPV and its derivatives [19–21]. The dynamic redshift is attributed to 'spectral' diffusion, whereby excitons excited on shorter chain segments hop to longer chain segments thereby reducing the exciton energy. In addition, studies of polarized luminescence from PPV chains found a time-integrated anisotropy of roughly 0.2, in agreement with our results [22]. These results imply that the exciton migration which leads to the decay of the anisotropy in our samples is the same process that is responsible for the spectral diffusion seen in previous work.

At excitation densities of $\sim 10^{19}$ cm$^{-3}$, the dynamics of the anisotropy changes completely. In this regime, the anisotropy of $PA_{EX}$ decays from an initial value of 0.35 to approximately 0.2 within several 100 fs. In addition, at 200 fs pump–probe delay time, the anisotropy continues to decrease as the excitation density is increased beyond the saturation density for singlet excitons ($\sim 10^{19}$ cm$^{-3}$), as shown in Fig. 5. Thus, in the regime above $10^{19}$ cm$^{-3}$, even though the density of excitons is not significantly increasing, the anisotropy after $\sim$200 fs continues to decrease. These data imply that a nonlinear mechanism(s) is activated at higher excitation densities which rapidly changes the spatial orientation of a significant portion of the singlet intrachain excitons.

The data of Fig. 2 show that the exciton population at approximately 200 fs pump–probe delay time saturates at an excitation density of $\sim 10^{19}$ cm$^{-3}$. A simple calculation shows that the density of monomers in the sample is in the order of $10^{21}$ cm$^{-3}$, assuming a film density of 1 gm/cm$^3$. Assuming the exciton wavefunction is spread over six monomer units [23,13], the exciton density should saturate at a few times $10^{20}$ cm$^{-3}$, if phase-space filling was the dominant factor limiting the exciton population density. The fact that the exciton density saturates at a density an order of magnitude below this value implies a longer range interaction dominates before phase-space filling becomes active. This long-range nonlinear interaction is consistent with a dipole-coupled Förster energy transfer process.

Two possible quadratic processes involving intrachain singlet excitons have been discussed as mechanisms leading to the generation of interchain charge separated excitations in phenylenevinylene oligomers [6]. The first is an Auger interaction (exciton–exciton annihilation) between two exci-

tons resulting in the promotion of one exciton to a higher excited state (biexciton). The biexciton possesses sufficient energy to overcome a potential barrier and decay into an interchain charge-separated excitation [6]. The second quadratic process is the sequential excitation of a chromophore by two photons from the same intense femtosecond pulse, again leading to a biexciton. This has been observed in polydiacetylene derivatives leading to ultrafast triplet excitons generation [24]. Although the data presented here do not distinguish between these two nonlinear mechanims, the ultrafast decay of the anisotropy at high excitation denisities implies that the creation of biexcitons leads not only to charge separation, but also to exciton hopping between different polymer chains or between segments of the same chain with a different spatial orientation. We thus conclude that there is a branching in the decay scheme of the biexcitons, with one branch leading to charge separation, and the other leading to exciton hopping.

## 5. Conclusion

We find a new PA peak in the TA spectrum of the soluble PPV derivative DP6-PPV. This feature peaks at roughly 0.5 eV and is due to transitions from intrachain excitons ($^1B_u$) to higher excited states ($^kA_g$). We find no evidence of a TA feature between 1.0 and 0.5 eV due to charge-separated photoexcitations. At high photoexcitation densities ($\sim 10^{19}$ cm$^{-3}$), we find that a nonlinear mechanism becomes important, leading to a dramatic increase in the rate of exciton hopping between chains.

## References

[1] D. Braun, A. Heeger, Appl. Phys. Lett. 58 (1991) 1982.
[2] J. Burroughes, D. Bradley, A. Brown, R. Marks, K. Mackay, R. Friend, P. Burns, A. Holmes, Nature 347 (1990) 539–541.
[3] F. Hide, M. DiazGarcia, B. Schwartz, M. Andersson, Q. Pei, A. Heeger, Science 273 (1996) 1833.
[4] N. Tessler, G. Denton, R. Friend, Nature 382 (1996) 695–697.
[5] N. Harrison, G. Hayes, R. Phillips, Phys. Rev. Lett. 77 (1996) 1881–1884.
[6] V. Klimov, D. McBranch, N. Barashkov, J. Ferraris, Phys. Rev. B 58 (1998) 7654.
[7] J. Hsu, M. Yan, T. Jedju, L. Rothberg, B. Hseih, Phys. Rev. B 49 (1994) 712–715.
[8] M. Yan, L. Rothberg, F. Papadimitrakopoulos, M. Galvin, T. Miller, Phys. Rev. Lett. 72 (1994) 1104–1107.
[9] B. Kraabel, V. Klimov, R. Kohlman, S. Xu, H.-L. Wang, D. McBranch, Phys. Rev. B 61 (2000) 8501.
[10] V. Klimov, D. McBranch, Opt. Lett. 23 (1998) 277.
[11] C. Cantor, P. Shimmel, Biophysical Chemistry, Freeman, San Francisco, 1980.
[12] S. Spagnoli, J. Berrear, C. Lapersonne–Meyer, M. Schott, J. Chem. Phys. 100 (1994) 6195.
[13] T. Hagler, K. Pakbaz, K. Voss, A. Heeger, Phys. Rev. B 44 (1991) 8652–8666.
[14] A. Dogariu, R. Gupta, A. Heeger, H. Wang, Synth. Met. 100, in press.
[15] Z. Vardeny, J. Tauc, Academic, Orlando, 1984.
[16] S. Frolov, W. Gellerman, M. Ozaki, K. Yoshino, Z. Vardeny, Phys. Rev. Lett. 78 (1997) 729.
[17] S. Xu, V. Klimov, B. Kraabel, H.-L. Wang, D. McBranch, in preparation.
[18] B. Kraabel, J. Hummelen, D. Vacar, D. Moses, N.S. Sariciftci, A.J. Heeger, F. Wudl, J. Chem. Phys. 104 (1996) 4267–4273.
[19] R. Kersting, U. Lemmer, R.F. Mahrt, K. Leo, H. Kurz, H. Bässler, E. Göbel, Phys. Rev. Lett. 70 (1993) 3820–3823.
[20] G. Hayes, I. Samuel, R. Phillips, Phys. Rev. B 52 (1995) 11569–11572.
[21] B. Schwartz, F. Hide, M. Andersson, A. Heeger, Chem. Phys. Lett. 265 (1997) 327–333.
[22] U. Rauscher, H. Bässler, E.O. Göbel, Phys. Rev. B 42 (1990) 9830.
[23] S. Graham, D. Bradley, R. Friend, C. Spangler, Synth. Met. 41 (1991) 12777.
[24] B. Kraabel, D. Hulin, C. Aslangul, C. Lapersonnemeyer, M. Schott, Chem. Phys. 227 (1998) 83.